Original Paper *Forma*, **17**, 321–338, 2002

A Method for Extraction of Bronchus Regions from 3D Chest X-ray CT Images by Analyzing Structural Features of the Bronchus

Takayuki KITASAKA[1]*, Kensaku MORI[2], Jun-ichi HASEGAWA[3] and Jun-ichiro TORIWAKI[1]

[1]*Department of Information Engineering, Graduate School of Engineering, Nagoya University, Furo-cho, Chikusa-ku, Nagoya 464-8603, Japan*
[2]*Research Center for Advanced Waste and Emission Management, Nagoya University, Furo-cho, Chikusa-ku, Nagoya 464-8603, Japan*
[3]*School of Computer and Cognitive Sciences, Chukyo University, Toyota 470-0393, Japan*
**E-mail address: kitasaka@toriwaki.nuie.nagoya-u.ac.jp*

(Received November 11, 2002; Accepted December 12, 2002)

Keywords: Bronchus, Chest X-ray CT Image, Volume of Interest, Sharpening Operation

Abstract. A method for extraction of bronchus regions from 3D chest X-ray CT images—by analyzing structural features of the bronchus—has been developed. This method enhances the bronchial walls by applying a sharpening operation and segments each bronchial branch by recognizing the tree structure from the trachea. It uses the volume of interest (VOI) to segment each branch. That is, the VOI is placed so as to envelope the branch currently being processed. The region growing is performed only inside the VOI so that each branch is extracted by a suitable threshold value. The final bronchus region is obtained by unifying the extracted branches. The new method was applied to three cases of 3D chest X-ray CT images. The experimental results showed that the method improved the extraction accuracy significantly compared to the previous method; that is, the average accuracy of segmentation was 82% for 4th-order, 49% for 5th-order, and 20% for 6th-order bronchi, compared to 45%, 16% and 3% by the previous method using the region-growing method with the constant threshold value.

1. Introduction

The human body consists of various organs, each with its own characteristic form. For example, the lung and the stomach have a form like a bag so that they can store, respectively, air or foods inside them. The bronchus has a tree structure for sending air to the whole lungs. It starts from the trachea as the root of a tree. The trachea bifurcates the left and the right main bronchus, which enter the left and the right lung. Bronchial branches are split repeatedly toward the peripheral of the lungs and, finally, connect with alveolus, where gas exchange takes place (NETTER, 1997).

From the view point of the diagnosis of the chest, the bronchus is a very important organ, since a lung disease such as a tumor is often concerned with the bronchus. For example, a tumor which draws the bronchi has a high suspicion of malignancy. The

diagnosis of the chest is usually done by observing CT images. However, because a CT image consists of dozens or more CT slices the diagnostic load on a medical doctor is heavy. Moreover, multi-slice CT scanners, which were developed in these days, produce hundreds of slices for a patient in seconds. This puts a further diagnostic load on the doctor. Development and utilization of a computer aided diagnosis (CAD) system to reduce this load has therefore been strongly desired (KATADA, 2000; TORIWAKI; 2003).

Many studies on automatically extracting bronchus regions from 3D chest X-ray CT images have been reported (MORI *et al.*, 1995; SONKA *et al.*, 1996; ISEKI *et al.*, 1997; TSUI and HENG, 2000; SCHLATHOELTER *et al.*, 2002). Conventional approaches are mostly based upon a region-growing method. Such so-called "region-growing" methods, however, can not extract particular bronchial branches influenced by the partial volume effect (PVE). In such cases, CT values for the air inside the bronchus lumen become higher and CT values for the bronchial walls become lower. This difference causes mis-segmentation of branches during the region-growing process. An optimal threshold value for each branch should be determined, and enhancement of bronchial walls will be required from above problems.

To meet this requirement, the concept of the "volume of interest" (VOI) is introduced to divide a given CT image into subimages that contain one bronchial branch in each subimage. Each bronchus region inside a subimage is segmented sequentially from the trachea, by extending the VOI in the direction that a bronchus runs, and by splitting it according to a bronchus branching. For each subimage, a sharpening operation based on the Laplacian filter is performed so as to enhance a bronchial wall that is weakened by the PVE. Another advantage of the proposed method is to provide the graph representation of the extracted bronchus tree simultaneously.

2. Problems of Bronchus Extraction

As mentioned above, conventional methods for bronchus extraction use a region-growing method (MORI *et al.*, 1995; SONKA *et al.*, 1996; ISEKI *et al.*, 1997; TSUI and HENG, 2000; SCHLATHOELTER *et al.*, 2002). It is reasonable that a region-growing method is used to segment a bronchus region, because the bronchial lumen that has low intensity are surrounded by the bronchial walls whose intensity are relatively high in a CT image. The growing method developed by MORI *et al.* (1995) can extract thick bronchi up to the 3rd-order from multi-slice CT images. However, the thickness of bronchial walls becomes thinner and thinner in peripheral area of the lung (NETTER, 1997), so their intensity becomes lower as shown in Fig. 1. Consequently, a hole appears in a bronchial wall in a CT image, due to the PVE. Holes often appear after the 4th-order branching level. Especially, a branch parallel to a CT slice is strongly influenced by PVE. Such branches cannot be segmented correctly by a region growing method since some leakages toward the outside of the bronchial lumen occur through the holes.

Some approaches to improve the accuracy of segmentation have been reported (ISEKI *et al.*, 1997; SCHLATHOELTER *et al.*, 2002). The method proposed by ISEKI *et al.* (1997) extracts a bronchus region by tracing the cross-sectional area of each bronchus. Bronchus regions on the cross-sectional area are segmented by the region-growing method with an adaptive threshold value. However this method does not take enhancement of the wall into account. Therefore parts of bronchi that were strongly influenced by the PVE cannot be

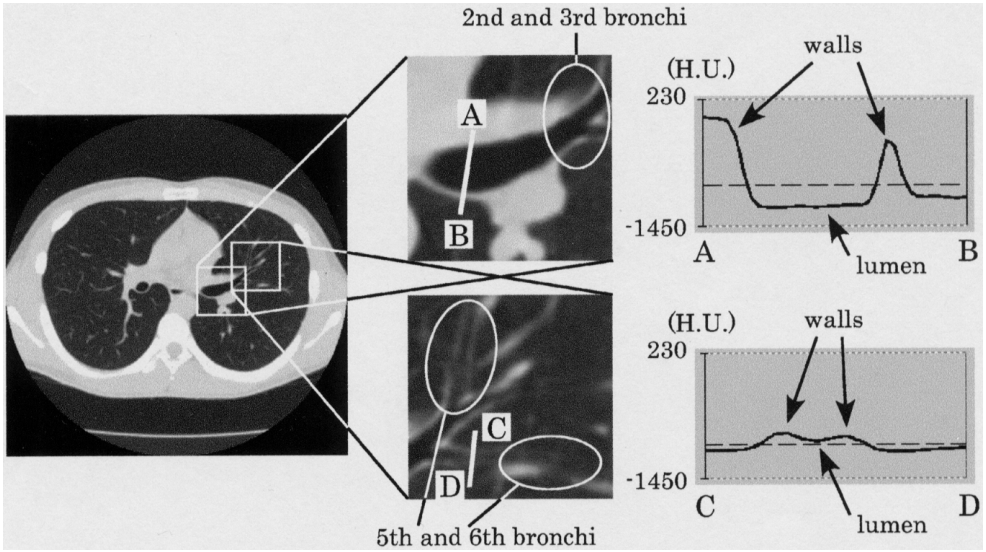

Fig. 1. An example of CT images. The left-side image shows a slice of the CT image; the right-upper and right-lower images are magnified images of the left-side image. Bronchial walls near the center side are strong (as indicated by white circles in the right-upper image). While, walls in the peripheral area (as shown by circles in the right-lower image) are very weak. The intensity profiles from A to B and C to D are also shown.

extracted or may be extracted incorrectly. The method of SCHLATHOELTER *et al.* (2002) employs a front propagation approach. During the segmentation process, the leakage can be detected by calculating the radius of an extracted lumen. Once the leakage is detected, the front at the leaked area is frozen; that is, the leaked area is excepted from the extraction result. This method is very fast and gives good results (60% of 5th-order bronchi can be segmented) from a multi-slice CT image with 0.68 mm isotropic resolution. However, the resolution of CT images used in practice is usually not isotropic, i.e., the z axis of the CT image has a coarser resolution than that of the x and y axes; therefore, this may cause the same problem described above.

Segmentation with an adaptive threshold value and enhancement of bronchial walls are key issues for improving extraction accuracy. The former requirement can be achieved by changing a threshold value of bronchus region extraction for each VOI, which contains only one bronchial branch. At a bifurcation point, VOI is split into two VOIs. Bronchi regions are segmented sequentially from the trachea, by extending the VOI in the direction of a branch (Fig. 2). The latter one is achieved by applying a sharpening operation based on the Laplacian filter to a VOI in order to mend holes.

The proposed method uses simple anatomical knowledge of the bronchus as follows:

(i) a branch has two or three child branches (bifurcation or trifurcation),

(ii) the diameters of branches become smaller with increasing bifurcations.

In the proposed method, prediction of branching directions of bronchi is not performed due to existence of many branching patterns.

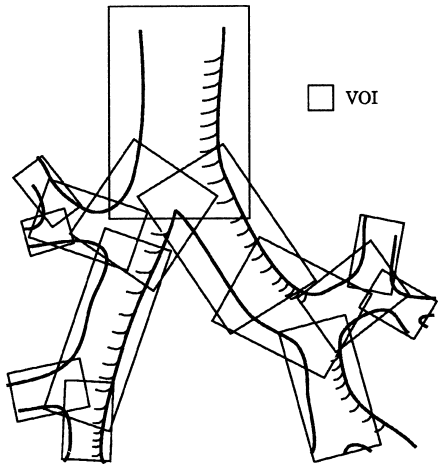

Fig. 2. Illustration of segmentation of bronchi by using VOIs. Bronchi are segmented sequentially from the trachea by the VOI, which divides a CT image into a subimage that contains one branch in it. Final bronchus region is obtained by unifying them.

3. Methodology

Figure 3 shows the flow chart of the proposed method. The method consists of seven steps: (1) rough segmentation of a bronchus region, (2) placement of a VOI for the trachea, (3) segmentation of a bronchus region in the VOI, (4) detection of bifurcation, (5) extension of the VOI, (6) modification of the direction of the VOI, and (7) placement of child VOIs. Final bronchus region is obtained by unifying bronchial branches extracted in each VOI.

3.1. VOIs and VOI images

A VOI determines a local processing area along with the direction of a bronchial branch. It is defined by three basis vectors, $\mathbf{e}_1$, $\mathbf{e}_2$ and $\mathbf{e}_3$, the position of the VOI's origin, $\mathbf{e}_0$, and the lengths along with basis vectors, l_1, l_2 and l_3 (Fig. 4(a)). Tri-cubic interpolation is utilized for generating a subimage from the original CT image. The direction $\mathbf{e}_3$ of a VOI is aligned to running direction of a bronchial branch. We call the direction of the vector $\mathbf{e}_3$ the direction of VOI. Also the length of a VOI means the length l_3 in this paper. Method for calculating $\mathbf{e}_1$, $\mathbf{e}_2$ and $\mathbf{e}_3$ is described in Subsec. 3.3. The three axes (*x*-, *y*-, and *z*-axis) of the subimage are parallel to the directions of the basis vectors (Fig. 4(b)). We generate a subimage where image resolution along each axis is identical, i.e., $u_x = u_y = u_z$. Actual values of u_x, u_y, and u_z are computed as follows. Let $U_{\min}$ (milli-meter) be the minimum resolution of a CT image and α be the magnification factor. Image resolution of a generated subimage (VOI image) is determined as

$$(u_x, u_y, u_z)=(U_{\min}/\alpha, U_{\min}/\alpha, U_{\min}/\alpha). \quad (1)$$

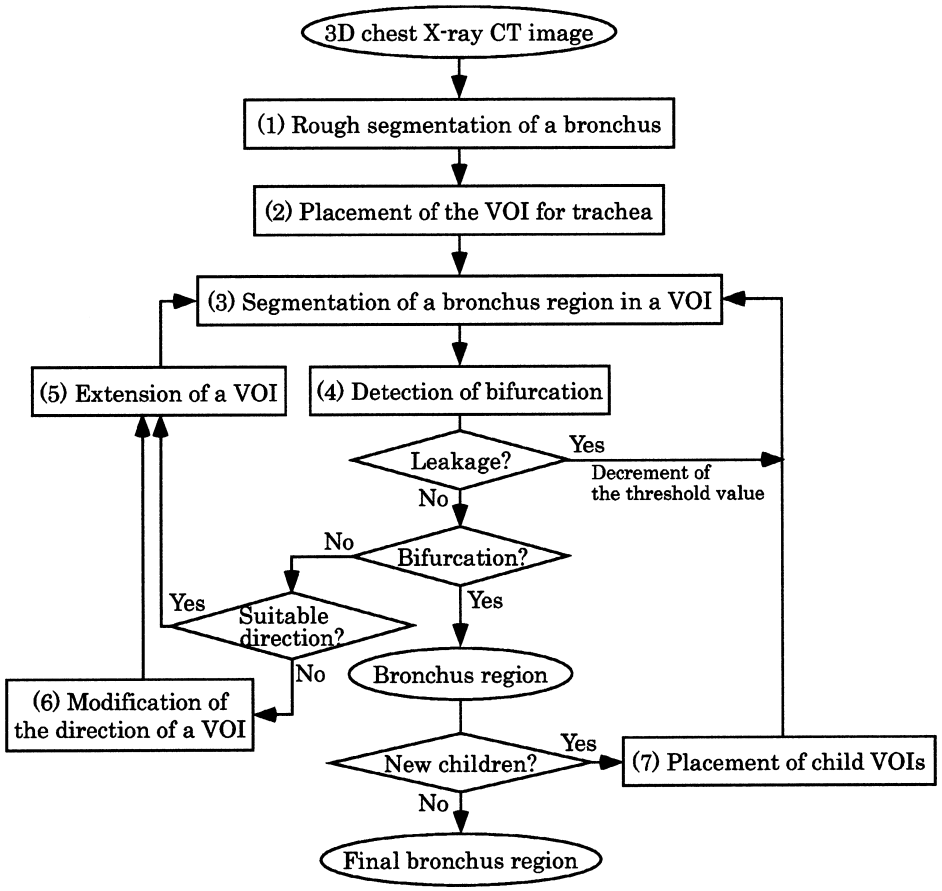

Fig. 3. The flow chart of the proposed method.

The magnification factor α is calculated as

$$\alpha = \left[10 * \frac{U_{\min}}{r} \right], \tag{2}$$

where [ ] expresses the Gauss sign, and r means the radius of a bronchial branch explained in the later section. This equation means the length l_i for each axis $\mathbf{e}_i$ has at least 20 voxels in a local coordinate system of a VOI. The subimage size (l_x, l_y, l_z) is given by

$$\left(l_x, l_y, l_z\right) = \left(\left[\frac{l_1}{u_x} \right] + 1, \left[\frac{l_2}{u_y} \right] + 1, \left[\frac{l_3}{u_z} \right] + 1 \right). \tag{3}$$

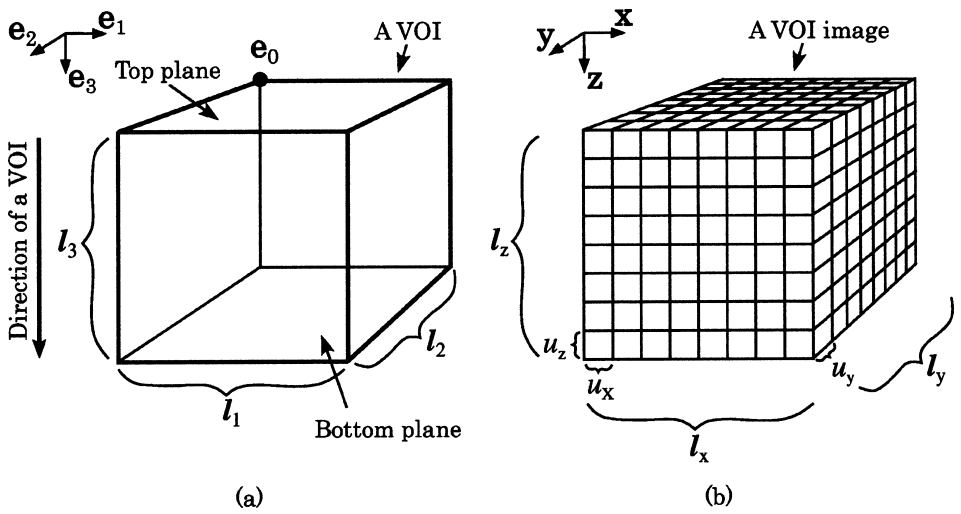

Fig. 4. Explanation of a VOI and a VOI image. (a) A local coordinate system of a VOI. It consists of the origin $\mathbf{e}_0$ and three basis vectors $\mathbf{e}_1$~$\mathbf{e}_3$. (b) A VOI image defined by a VOI of (a). Each voxel of a VOI image is calculated by interpolating a given CT image with isotropic resolution.

In general, slice spacing is wider than pixel spacing. A branch parallel to a CT slice may be split into separated regions by the PVE as shown in Fig. 5(a). The interpolation process for generating isotropic image helps to connect regions which are forced to be separated by PVE (Fig. 5(b)).

3.2. Enhancement of VOI image

The sharpening operation based on the Laplacian of Gaussian (LoG) filter is applied to enhance bronchial walls weakened by the PVE. First, the VOI image denoted by $\mathbf{F} = \{f_{ijk}\}$ is smoothed by a three dimensional gray-level closing operation whose element function has a sphere shape (HARALICK *et al.*, 1987). The radius of the sphere is equivalent to the size of a voxel of a subimage (u_x, u_y, u_z). The sharpened image, $\mathbf{F}_{\text{sharpen}}$, of $\mathbf{F}$ is given by

$$\mathbf{F}_{\text{sharpen}} = \mathbf{F} - \beta \text{LoG}(\mathbf{F}) \quad (\beta > 0), \tag{4}$$

where LoG($\mathbf{F}$) is an output of the LoG filter for an input $\mathbf{F}$, and β is a coefficient of the sharpening operation. The subtraction between images, $\mathbf{F} - \mathbf{G}$, represents the set of the subtraction, $\{f_{ijk} - g_{ijk}\}$. An output of the Laplacian filter of $\mathbf{F}$ at the point (i, j, k), denoted by $\text{L}(\mathbf{F})|_{ijk}$, is expressed by

$$\text{L}(\boldsymbol{F})\big|_{ijk} = -26 f_{ijk} + \sum_{(p,q,r)\in\mathcal{N}_\alpha(i,j,k)} f_{pqr}, \tag{5}$$

$$\mathcal{N}_\alpha(i,j,k) = \left\{(i+\alpha p, j+\alpha q, k+\alpha r);\ \max\left\{|p|,|q|,|r|\right\} = 1\right\} \tag{6}$$

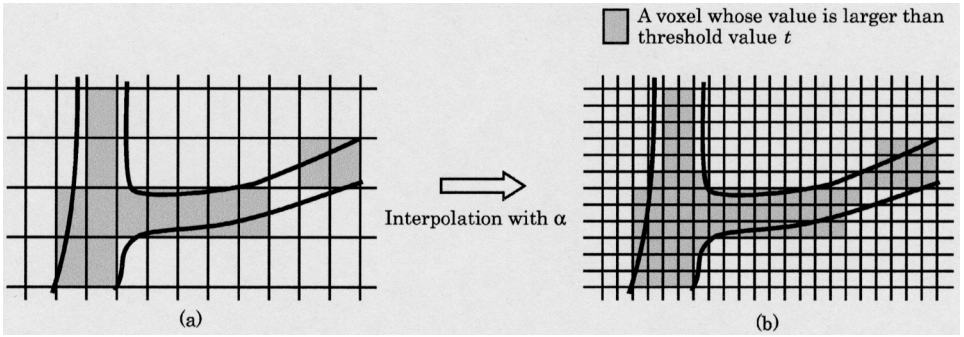

Fig. 5. Illustration of the effect of the interpolation with isotropic resolution. (a) An original cross section of bronchi. A branch is split by the PVE. (b) Cross section after interpolation with isotropic resolution. The split branch can be connected.

where $\mathcal{N}_\alpha(i, j, k)$ represents α-neighborhood of the point (i, j, k). The Laplacian filter outputs a negative value when neighboring points have relatively lower values than the processing point but it outputs a positive value when neighboring points have higher. Voxels inside the bronchial lumen thus tend to have positive values after Laplacian operation, and voxels on the bronchial walls (edge) tend to have negative values. However, since ridge-type edges may be weakened by the Laplacian filter when intensities of regions neighboring to the edges are higher than the intensities of the edges itself, the Laplacian filtering process may weaken the CT values of the bronchial wall which has higher values than the values of the lumen. Figure 6(b) shows an example of such undesirable outputs in two dimensional case. Therefore, we use the sharpening operation defined by the following Eq. (7) for avoiding this problem.

$$\mathbf{F}_{\text{sharpen}} = \mathbf{F} - \beta(\gamma \text{LoG}(\mathbf{F}) + (1 - \gamma)\text{L}'\text{oG}(\mathbf{F})), \tag{7}$$

where L′ is the modified Laplacian filter and γ is the weight of LoG and L′oG. The mask shape of L′ is basically identical to L. The filter L′ excepts voxels which has greater values than the value of the center voxel of the mask from its own mask. The L′ filter is given by

$$\text{L}'(\mathbf{F})\big|_{ijk} = -N_{\text{lower}} f_{ijk} + \sum_{(p,q,r)\in\mathcal{N}_\alpha(i,j,k)} \begin{cases} f_{pqr} & \left(f_{pqr} < f_{ijk}\right) \\ 0 & (\text{otherwise}), \end{cases} \tag{8}$$

where N_{lower} is the number of neighboring points that satisfy $f_{pqr} < f_{ijk}$. The output of L′ is always negative value; that is, the intensities after the sharpening by L′ never decrease (Fig. 6(c)), though the voxels inside the lumen are enhanced. The parameter γ controls the degree of intensity enhancement. This filtering process raise CT values of the bronchial wall and reduce CT values inside the bronchial lumen.

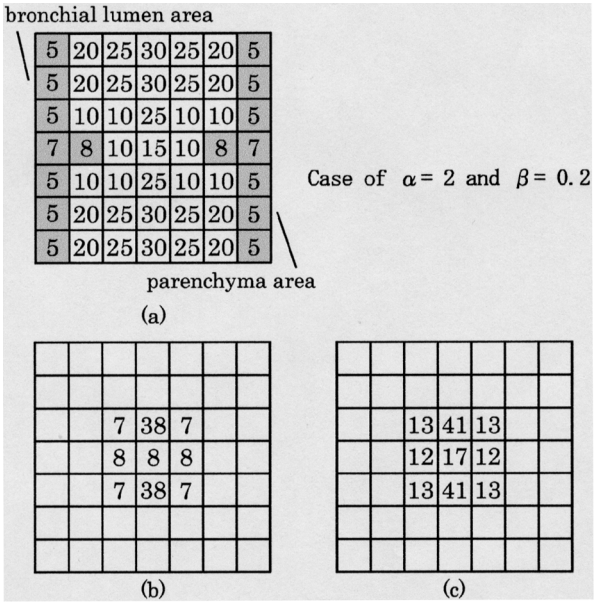

Fig. 6. An example of outputs of the sharpening operation by L and L′ in two dimensional case. Assume that pixels whose values are less than 10 are air regions, and that parameters α and β in Subsec. 3.1 are 2 and 0.2, respectively. (a) A gray-level picture. Ridge-type wall is formed. (b) Outputs of the sharpening by L. The center pixel, which has relatively high intensity than lumen pixels, is weakened down to 8 (lumen intensity). (c) Outputs of the sharpening by L′. Unlike L, the center pixel is enhanced well. This may happen also in three dimensional case.

3.3. Detailed procedures for bronchus extraction

Step (1) Rough segmentation of a bronchus region

A bronchus region is segmented roughly by the method previously developed by MORI *et al.* (1995). The threshold value T_{ini} determined by the MORI's method is used for the basic threshold value to segment each bronchial branch.

Step (2) Placement of the VOI for trachea

The trachea region on the top slice of a CT image is obtained from the bronchus region extracted in Step (1). The center of gravity of the trachea region, $\mathbf{c}_{\text{top}}$, and the radius, $r_{\text{top}} = \sqrt{S_{\text{top}} / \pi}$, are calculated, where S_{top} is the area (number of pixels) of the trachea region on the top slice of a CT image. The VOI for the trachea is initially determined by a cube whose edge length is five times of r_{top}. The center of the top plane of the VOI is $\mathbf{c}_{\text{top}}$. The directions of the axes of the VOI are parallel to those of the CT image; i.e., $\mathbf{e}_3$ turns to the axial direction.

Step (3) Segmentation of a bronchus region in a VOI

A bronchus region in the VOI image is extracted by applying the region-growing method (MORI *et al.*, 1995). The seed points of the growing process for the trachea are pixels of the trachea region obtained in Step (2). For bronchial branches after the trachea, voxels of extracted bronchus region of the parent branch inside the current VOI are used

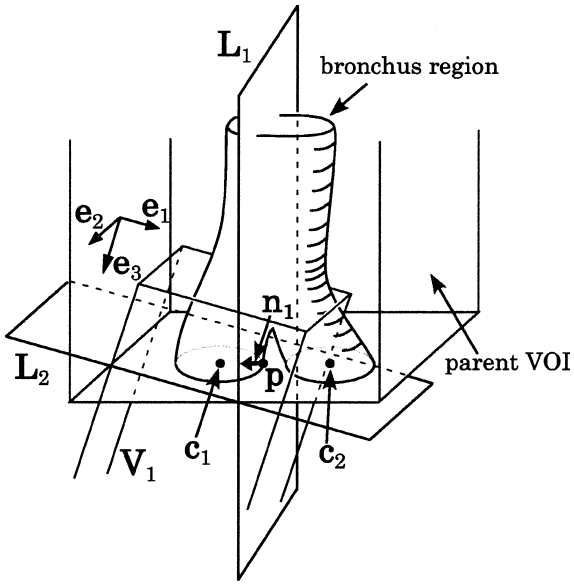

Fig. 7. Illustration of levees. Plane L_1 prevents extraction of sibling branches and the plane L_2 prohibits growing toward the parent branch.

as seeds. The trachea, the right, and the left main bronchus are extracted by using the constant threshold value $t_{\text{ini}} + 100$ to reduce computation time, since their bronchial walls are suffciently thick and have higher CT values. For other branches, a suitable threshold value t that satisfies conditions (I) and (II) described in Step (4) is found by a binary search algorithm. The upper threshold limit t_{upper} and the lower limit t_{lower} are $t_{\text{ini}} + 100$ and –1200 H.U. (Hounsfield Unit), respectively.

In the growing process, two levees (planes) are set to prevent the reverse growing toward parent and sibling branches as shown in Fig. 7. Let us consider that the current VOI is V_1 including the point $\mathbf{c}_1$. The levee L_1 is given by

$$n_{1x}x + n_{1y}y + n_{1z}z + \mathbf{n}_1 \cdot \mathbf{p} = 0, \tag{9}$$

where $\mathbf{n}_1 = (n_{1x}, n_{1y}, n_{1z})$ is the unit vector of $\mathbf{c}_2 - \mathbf{c}_1$. Points $\mathbf{c}_1$ and $\mathbf{c}_2$ are centers of gravity of branched bronchus regions on the surface of the parent VOI image. The point $\mathbf{p}$ is the nearest point to $\mathbf{c}_2$ on the surface of the VOI image. The other levee L_2 is defined by

$$e_{3x}x + e_{3y}y + e_{3z}z + \mathbf{e}_3 \cdot \mathbf{c}_1 = 0. \tag{10}$$

No voxels beyond the levees are extracted.

Step (4) Detection of bifurcation

Bifurcation is detected by analyzing the number of connected components on the surface of the VOI image. First, extracted bronchial voxels on the surface of the VOI image

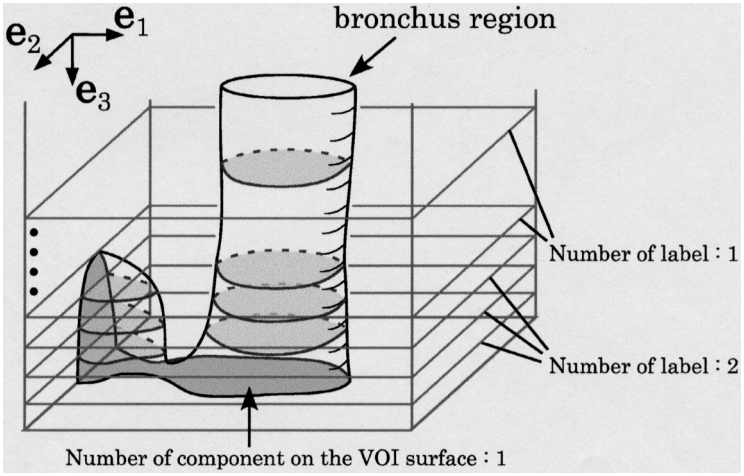

Fig. 8. An example of leakage detection. Leakage is detected in this case since there are two components on cross sections of the VOI image, despite the number of component on the surface of the VOI, N_c, is one.

are classified by three dimensional labeling process, and the number of voxels for each label, S_i ($1 \leq i \leq N_c$), is measured. If S_i is smaller than $S_{\max}/S_{\text{ratio}}$, it is eliminated by regarding as the shape noise and N_c is decremented. Here $S_{\max}$ denotes the number of voxels of the maximum component of S_i. The value S_{ratio} is a threshold value for elimination of small components.

The leakage beyond the bronchial wall is detected by checking the extracted region in the VOI image. In the case of normal bifurcation, the bronchus never splits backward in the direction of the VOI, $\mathbf{e}_3$. Hence, if N_c is one or larger (i.e., possibility of bifurcation), the following conditions are checked (Fig. 8);

(I) N_c is less than four (from knowledge (i)),

(II) the number of components on each cross section of the VOI image is at most N_c or less.

If any of the conditions (I) and (II) is not satisfied, the leakage is detected. When the leakage occur the upper limit of the threshold, t_{upper}, is decremented by Δt H.U. and Step (3) is processed again. If above conditions are satisfied and N_c is two or three, bifurcation (or trifurcation) is detected. Then it progresses to Step (7). If N_c is zero, the extraction process is finished and bronchi after the current one are not searched.

Otherwise ($N_c = 1$), the direction of the VOI is checked before extending the VOI. The center of gravity of the extracted regions on the surface of the VOI image is calculated. If the length between the center of gravity and the center of the bottom plane of the VOI is larger than ε, Step (6) is processed in order to make the direction of the VOI coincident with that of a bronchus. Step (5) is then performed.

Step (5) Extension of a VOI

The length of the VOI, l_3, is extended by one voxel and the VOI image is re-calculated. After the extension of the VOI, Step (3) is processed again.

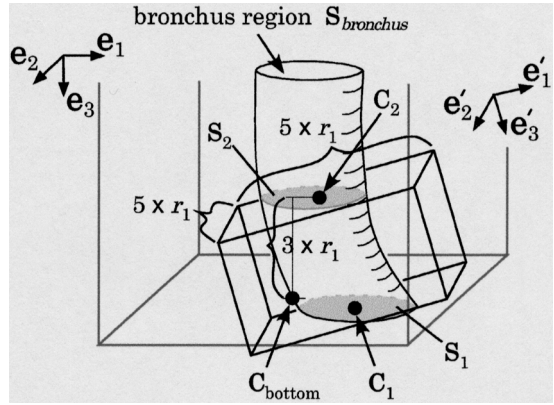

Fig. 9. Modification of the VOI. The direction of the VOI is modified so as to coincide with that of the bronchial branch. The modified VOI size is calculated based on r_1, which is the mean radius of the branch.

Step (6) Modification of the direction of a VOI

When there is the difference between the direction of the VOI and that of the bronchial branch, the direction of the VOI is modified so as to coincide with that of the branch. Let S_1, $\mathbf{C}_1$, and r_1 be the extracted bronchus region on the bottom plane of the VOI image, the center of gravity of S_1, and the radius of the bronchus region, respectively (Fig. 9). The radius r_1 is given as the mean radius of the branch,

$$r_1 = \sqrt{\frac{S_{\text{bronchus}}}{l_3 \pi}}, \tag{11}$$

where S_{bronchus} denotes the volume (number of voxels) of extracted bronchus region in the VOI. The coordinate system of the modified VOI, ($\mathbf{e}_1'$, $\mathbf{e}_2'$, $\mathbf{e}_3'$), is calculated by

$$\mathbf{e}_3' = \frac{\mathbf{C}_1 - \mathbf{C}_2}{\|\mathbf{C}_1 - \mathbf{C}_2\|}, \tag{12}$$

$$\mathbf{e}_1' = \mathbf{e}_3' \times \mathbf{e}_3, \tag{13}$$

$$\mathbf{e}_2' = \mathbf{e}_3' \times \mathbf{e}_1', \tag{14}$$

where $\mathbf{C}_2$ is the center of gravity of the extracted bronchus area on the $(l_3 - 3r_1)$-th cross section of the VOI image as shown in Fig. 9*. The sign "×" means the outer product of vectors. The center of the top plane of the modified VOI is $\mathbf{C}_2$. The size of it, (l_1, l_2, l_3), is

*If $3r_1$ is larger than l_3, l_3 is used for calculating $\mathbf{C}_2$ instead of $3r_1$.

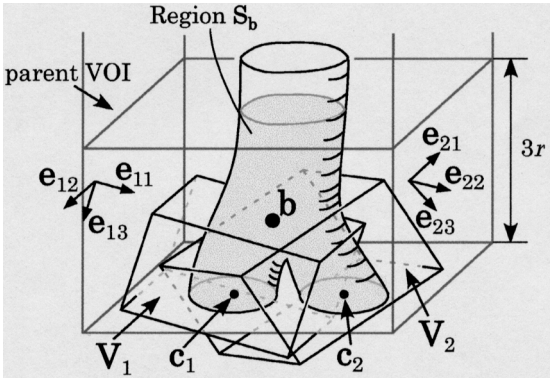

Fig. 10. Illustration of the initialization process for child VOIs. VOIs V_1 and V_2 are arranged according to bifurcation point b and the centers of gravity of components $\mathbf{c}_1$ and $\mathbf{c}_2$.

given by $(5r_1, 5r_1, \|\mathbf{C}_1 - \mathbf{C}_2\|)$. After modification, Step (5) is processed to segment further bronchus region.

Step (7) Placement of child VOIs

If bifurcation is detected in Step (4), child VOIs for child bronchi are placed by the following steps (Fig. 10). The mean radius of the extracted bronchus region, r, is obtained by the same manner with the calculation of r_1 in Step (6). The branching point, $\mathbf{b}$, is given as the center of gravity of the region S_b in Fig. 10. Centers of gravity, $\mathbf{c}_i$, of components S_i on the surface of the VOI image detected in Step (4), are also measured. The branching directions of child bronchi are then determined as $\mathbf{c}_i - \mathbf{b}$. The coordinate system of the child VOIs, $(\mathbf{e}_{i1}, \mathbf{e}_{i2}, \mathbf{e}_{i3})$ are calculated by

$$\mathbf{e}_{i3} = \frac{\mathbf{c}_i - \mathbf{b}}{\|\mathbf{c}_i - \mathbf{b}\|}, \tag{15}$$

$$\mathbf{e}_{i1} = \mathbf{e}_{i3} \times \mathbf{e}_3, \tag{16}$$

$$\mathbf{e}_{i2} = \mathbf{e}_{i3} \times \mathbf{e}_{i1}. \tag{17}$$

The center of the top plane of child VOIs is $\mathbf{b}$. The size of child VOIs, (l_{i1}, l_{i2}, l_{i3}), are given by $(5r, 5r, \|\mathbf{c}_i - \mathbf{b}\|)$, while l_1 is used instead of $5r$ if $5r > l_1$ (from knowledge (ii)). The bronchus region that have been extracted in the current VOI is added to the final bronchus region. Then, Steps (3)~(6) are repeated to extract subsequent branches.

4. Experiment

Three cases of 3D chest X-ray CT images were used in the experiment. The acquisition parameters of these CT images are listed in Table 1. We segment bronchus regions by the

Table 1. Acquisition parameters of CT images.

Case	Number of pixels in a slice	Pixel size (mm)	Number of slices	Slice thickness (mm)	Slice interval (mm)
1		0.625×0.625	350	2.0	1.0
2	512×512	0.546×0.546	252	2.0	1.0
3		0.586×0.586	156	2.0	2.0

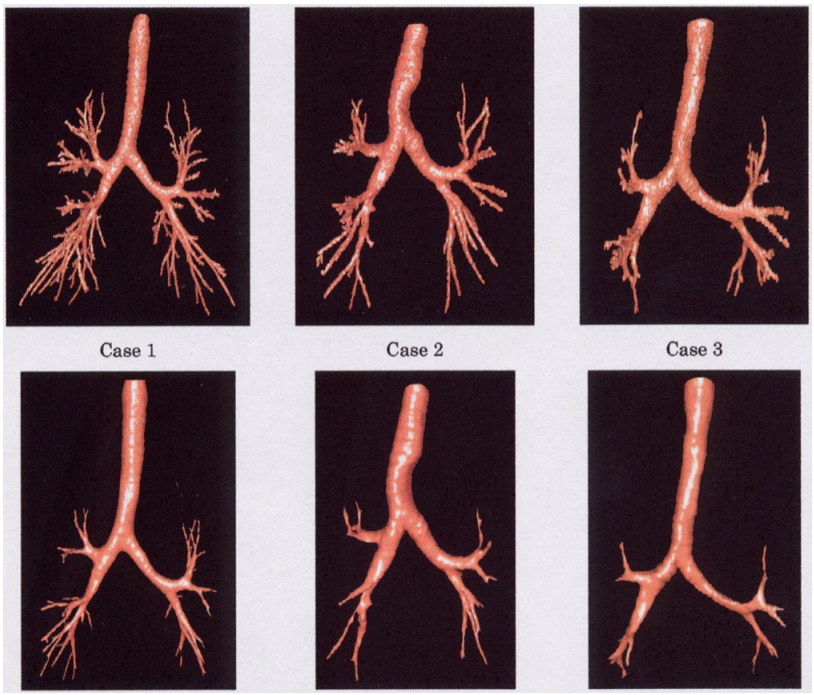

Fig. 11. Three dimensional views of the extracted bronchus region by the proposed method (upper row) and the method described in the reference (MORI *et al.*, 1995) (lower row).

proposed method, the previous method (MORI *et al.*, 1995) without the interpolation nor the sharpening, by the previous one with the interpolation or the sharpening, and by the one with both the interpolation and the sharpening to evaluate their effect. The experiment was repeated and the coefficient value β was varied from 0.05 to 0.3 each time. The values of γ, S_{ratio}, Δt, and ε were set to 0.5, 15, 4, and $l_1/6$, respectively.

4.1. Experimental results

Figures 11, 12, 13 and 14 show examples of extracted results. Figure 12 shows extracted tree structure. The new method can extract the tree structure just by linking each

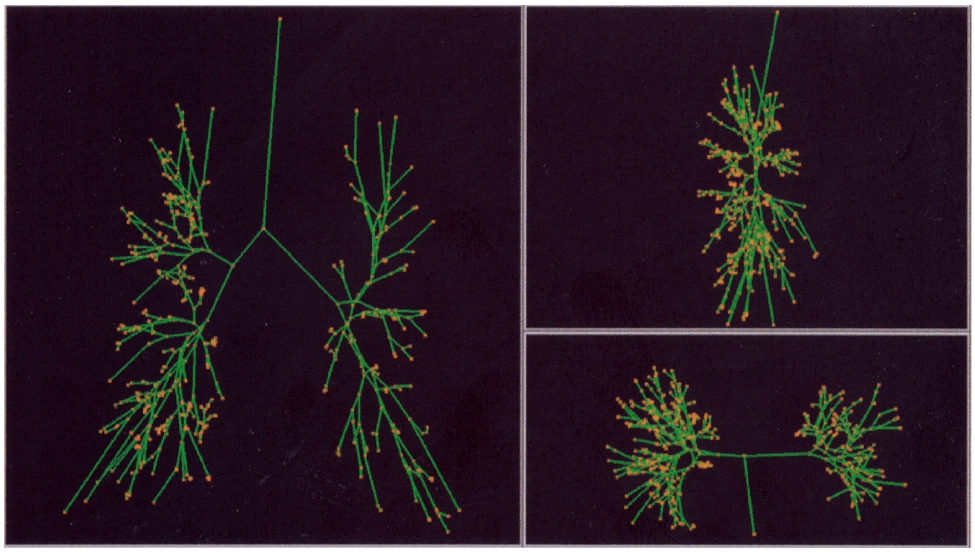

Fig. 12. Examples of the extracted tree structure of the bronchus for Case 1 ($\beta = 0.15$). The left-side, right-upper, and right-lower images are the images when seeing from the front, the right, and the top of human body.

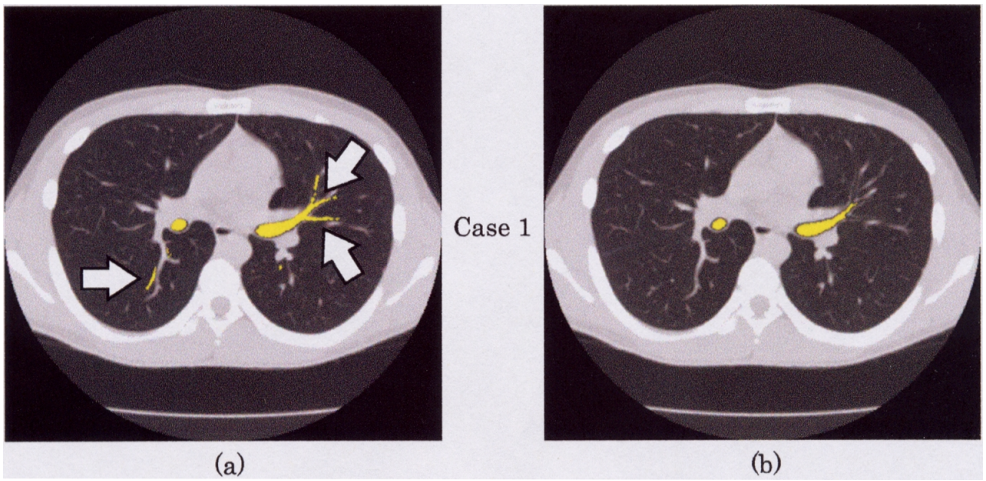

Fig. 13. Examples of the improvement of extraction results. This image is same slice in Fig. 1. Branches that accompany the CT slice can be segmented by the proposed method (white arrows).

Table 2. Comparison of the number of bronchi and leakages (false branches) extracted by the proposed method and the previous method (MORI *et al.*, 1995). Terms "I" and "S" mean interpolation and sharpening, respectively.

Case	Number of extracted bronchi						Number of leaks (false branches)			
	Proposed method			Previous method			Proposed method			Previous method
	β: 0.05	0.15	0.3	w/o I nor S	w/I	w/I and S	β: 0.05	0.15	0.3	
1	222	244	246	92	101	134	9(4)	15(8)	22(34)	0(0)
2	101	123	131	46	54	64	0(0)	6(2)	10(11)	0(0)
3	65	83	90	32	38	38	2(7)	5(5)	12(15)	0(0)

Table 3. Comparison of the extraction accuracies for each order of branches by the proposed method and the previous one with interpolation and sharpening.

Case	Number of extracted bronchi	
	Proposed method β: 0.15	Previous method w/I and S
1		
4th	40/41 (98%)	30/41 (73%)
5th	64/82 (78%)	35/82 (43%)
6th	75/164 (46%)	12/164 (7%)
2		
4th	34/42 (81%)	20/42 (45%)
5th	39/84 (46%)	4/84 (5%)
6th	18/168 (11%)	1/168 (1%)
3		
4th	28/42 (67%)	8/42 (19%)
5th	20/84 (24%)	0/84 (0%)
6th	2/168 (2%)	0/168 (0%)

bifurcation point without performing any additional process such as the thinning process. Arrows in Fig. 13 indicate examples of additionally segmented branches by the proposed method. The number of bronchial branches extracted by the previous and the proposed methods is listed in Table 2. It is clear that the proposed method can segment a much larger number of bronchi than the previous method. The extraction accuracies for the 3rd, 4th, and 5th-order bronchi were also evaluated by an author (Table 3)*. Here the accuracy is defined by

$$\text{Accuracy} = \frac{\text{Number of extracted branches}}{\text{Number of branches that can be observed on a CT image}}. \tag{18}$$

The average accuracy among three cases for the 4th-order bronchi was improved by 37%,

*Definition of the branching order of bronchial branches is given in Appendix with their numbers.

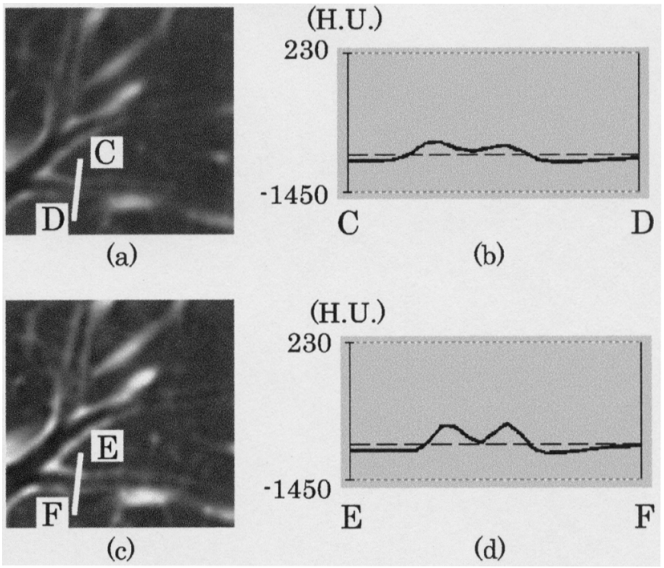

Fig. 14. An example of the sharpened image. (a) Original image (same part in Fig. 1). (b) Intensity profile from C to D in (a). (c) Sharpened image of (a). (d) Intensity profile from E to F in (c).

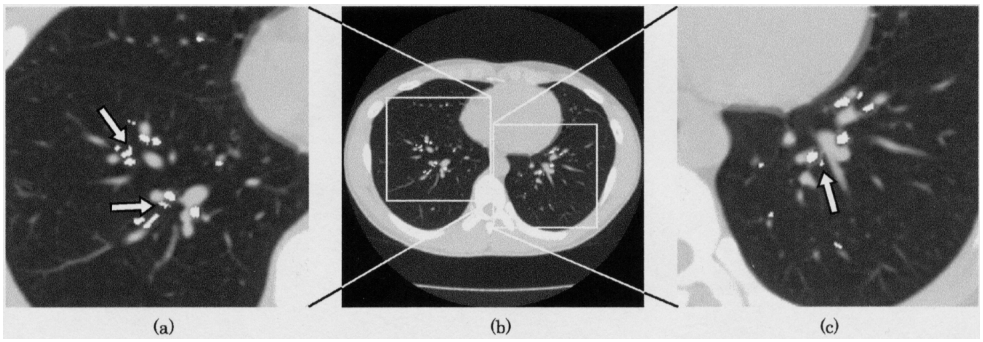

Fig. 15. Examples of deterioration of extraction results. Small leakages occurred (white arrows).

that for the 5th-order bronchi by 33%, that for the 6th-order bronchi by 17%. The computation time is about one hour for Case 1, about forty minutes for Case 2, and about twenty minutes for Case 3 (CPU: AMD Athlon 1900+).

4.2. Discussion

As seen in Tables 2 and 3 and Figs. 11 and 13, the proposed method can segment a large number of thinner bronchi than the previous method. The remarkable effectiveness of the

interpolation, the sharpening operation, and segmentation with an adaptive threshold value by using VOIs was revealed in the experiment.

Regarding the effect of the interpolation and the sharpening operation, the number of segmented bronchi increases according to apply the interpolation and the sharpening operation before executing the region-growing (MORI *et al.*, 1995) as shown in Table 2. This is because the apparent connectivity of voxels is improved by the interpolation and bronchial walls are enhanced by the sharpening operation. An example of the effect of the sharpening operation is given in Fig. 14. The bronchial walls are enhanced and the intensity contrast between the bronchial lumen and walls becomes higher. The interpolation and the sharpening operation are of importance for pre-processing of bronchus extraction.

The extraction accuracy of the proposed method (after the 5th-order bronchi) is significantly higher than that of the previous method (Table 3). Since CT values for the lumen of bronchial branches influenced by the PVE are higher value than those for thick branches, the region-growing method with the constant threshold fails to extract them. The proposed method segments each bronchial branch sequentially from the trachea by using the VOIs, so that such branches can be extracted with proper threshold values. For Case 1, 98% of 4th-order, 78% of 5th-order, and 46% of 6th-order bronchi can be segmented.

However, the coefficient β for the sharpening operation closely relates to the occurrence of leakage as shown in Table 2 and Fig. 15. When β is larger value i.e., $\beta = 0.3$, voxels that are not actually bronchial walls, e.g., noise voxels, are also enhanced. Small leakage areas that contain short false branches are consequently extracted as bronchi. Reversely, a smaller value of β such as $\beta = 0.05$, cannot enhance bronchial walls effectively. The number of leakages can be decreased, while that of segmented bronchi is also reduced. Child VOIs are not generated unless the bifurcation is detected, even if incorrect extraction takes place. The number of false branches may become smaller in this case (Table 2). The experiment showed that the most suitable value of β is 0.15. To eliminate such small leakages, the post-processing may be necessary.

High computation time due to the one-by-one extension of a VOI should be also improved. One of possible improvement is to predict the direction and the length of child bronchi by using further anatomical knowledge such as the length of each branch and bifurcation angles of child branches. The existence of singular branching patterns, however, must be considered carefully.

5. Conclusion

We developed a method to extract bronchus regions from 3D chest X-ray CT images by using structural features of the bronchus. This method extracted each bronchial branch by tracing the bronchial tree by using the VOIs. The bronchial walls were enhanced by the sharpening operation during segmentation. The interpolation and the sharpening operation of the original CT image were indispensable as pre-processing of bronchus extraction. Adaptive thresholding by using VOIs significantly improved the accuracy of segmentation. That is, the average accuracy of segmentation was 82% for 4th-order, 49% for 5th-order and 19% for 6th-order bronchi. However, there remains possibility of generating false branches due to leakages in the periphery of lung. Future work includes the further experiment using much larger number of CT images, the automatical determination of β in

the sharpening operation, development of the post-processing to eliminate leaked areas, automatical anatomical labeling of bronchi, the reduction of computation time, and more detailed comparison of the performance with other methods by Schlathoelter and others.

Appendix

We adopt the definition of branching order of bronchi described in the reference (NETTER, 1997) as follows:

- 0th order: the trachea (1 branch),
- 1st order: right and left main bronchus (2),
- 2nd order: right upper lobar bronchus, right intermediate lobar bronchus, right inferior bronchus, right middle lobar bronchus, left superior lobar bronchus, left superior division bronchus, left lingular bronchus, left inferior lobar bronchus (8),
- 3rd order: right B1 (RB1), RB2, RB3, RB4, RB5, RB6, RB7, RB8, RB9, RB10, left B1+2 (LB1+2), LB3, LB4, LB5, LB6, LB7+8, LB9, LB10 (18),
- 4th order: RB1a, RB1b, RB2a, RB2b, RB3a, RB3b, RB4a, RB4b, RB5a, RB5b, RB6a, RB6b, RB6c, RB7a, RB7b, RB8a, RB8b, RB9a, RB9b, RB10a, RB10b, RB10c, LB1+2a, LB1+2b, LB1+2c, LB3a, LB3b LB3c, LB4a, LB4b, LB5a, LB5b, LB6a, LB6b, LB6c, LB7+8a, LB7+8b, LB9a, LB9b, LB10a, LB10b, LB10c (42).

The authors thank Dr. S. Nawano of National Cancer Center Hospital East Japan, Dr. Hiroshi Natori of Sapporo Medical University, Dr. Masaki Mori of Sapporo Kousei Hospital, Dr. Hirotsugu Takabatake of Minami-ichijyo Hospital and Dr. Hedeaki Otsuji of Saisei Suita Hospital for providing the experiment samples. They also thank the members of our laboratory at Nagoya University for their collaboration. This work was supported in part by the Grant-in-Aid for Scientific Research for Private University High-Tech Research Center provided by the Ministry of Education, Culture, Sports, Science and Technology of the Japanese government and the Grant-in-Aid for Cancer Research from the Ministry of Health, Welfare and Labor of the Japanese government.

REFERENCES

HARALICK, R. M., STERNBERG, S. R. and ZHUANG, X. (1987) Image analysis using mathematical morphology, *IEEE Trans. on PAMI*, **9**, 4, 532–550.

ISEKI, F., KOBATAKE, H., OMATSU, H. and KAKINUMA, R. (1997) A new method to extract three dimensional tree structures of bronchus from chest CT images, *IEICE D-II*, **J80-D-II**, 10, 2841–2847 (in Japanese).

KATADA, K. (2000) Multi slice CT and CAD, *CADM News Letter*, **29**, 10–12 (in Japanese).

MORI, K., HASEGAWA, J., TORIWAKI, J., ANNO, H. and KATADA, K. (1995) Automated extraction and visualization of bronchus from 3D CT images of lung, *Proc. of 1st International Conference on Computer Vision, Virtual Reality and Robotics in Medicine (CVRMed'95)*, pp. 542–548.

NETTER, F. H. (1997) Atlas of human anatomy, in *NOVARTIS*, 2nd Ed., PLATE 190–193.

SCHLATHOELTER, T., LORENZ, C., CARLSEN, I. C., RENISCH, S. and DESCHAMPS, T. (2002) Simultaneous segmentation and tree reconstruction of the airways for virtual bronchoscopy, *Proc. of SPIE on Medical Imaging 2002*, **4684**, pp. 103–113.

SONKA, M., PARK, W. and HOFFMAN, E. A. (1996) Rule-based detection of intrathoracic airway trees, *IEEE Trans. on Medical Imaging*, **15**, 3, 314–326.

TORIWAKI, J. (2003) Forty years of CAD, *IEEE Trans. on Medical Imaging* (in print).

TSUI, Y. L. and HENG, P. A. (2000) Automated extraction of bronchus from 3D CT images of lung based on generic algorithm and 3D region growing, *Proc. of SPIE on Medical Imaging 2000*, **3979**, pp. 906–916.